© 2015. Published by The Company of Biologists Ltd | Development (2015) 142, 1242-1253 doi:10.1242/dev.115386

RESEARCH ARTICLE

STEM CELLS AND REGENERATION

Pericytes in the myovascular niche promote post-natal myofiber growth and satellite cell quiescence

Enis Kostallari[1,2], Yasmine Baba-Amer[1,3], Sonia Alonso-Martin[1,3], Pamela Ngoh[1,4], Frederic Relaix[1,3,5,6,7], Peggy Lafuste[1,3,*] and Romain K. Gherardi[1,3,7,*,‡]

ABSTRACT

The satellite cells, which serve as adult muscle stem cells, are both located beneath myofiber basement membranes and closely associated with capillary endothelial cells. We observed that 90% of capillaries were associated with pericytes in adult mouse and human muscle. During post-natal growth, newly formed vessels with their neuroglial 2 proteoglycan (NG2)-positive pericytes became progressively associated with the post-natal muscle stem cells, as myofibers increased in size and satellite cells entered into quiescence. *In vitro*, human muscle-derived pericytes promoted myogenic cell differentiation through insulin-like growth factor 1 (IGF1) and myogenic cell quiescence through angiopoietin 1 (ANGPT1). Diphtheria toxin-induced ablation of muscle pericytes in growing mice led both to myofiber hypotrophy and to impaired establishment of stem cells quiescence. Similar effects were observed following conditional *in vivo* deletion of pericyte *Igf1* and *Angpt1* genes, respectively. Our data therefore demonstrate that, by promoting post-natal myogenesis and stem cell quiescence, pericytes play a key role in the microvascular niche of satellite cells.

KEY WORDS: Pericytes, Post-natal development, Satellite cell differentiation, Satellite cell quiescence, Skeletal muscle, Mouse, Human

INTRODUCTION

Stem cells reside in specialized environments that regulate their behavior, called stem cell niches. Myogenic stem cells called satellite cells (mSCs) are involved in muscle growth and in regeneration following injury. During the late fetal development period, a basal lamina forms around myofibers (Bröhl et al., 2012; Rosen et al., 1992) and myogenic cells expressing PAX7 and PAX3 adopt the mSC position between the basal lamina and plasma membrane of myofibers (Relaix et al., 2005). mSCs have the potential to provide additional myonuclei to the myofiber or to enter a quiescent state. The mSC fate is tightly regulated by dynamic interplays between mSC intrinsic factors and extrinsic factors constituting the mSC niche (Yin et al., 2013). In undamaged adult muscle, mSCs are quiescent, binding the basal lamina through α7/β1 integrin and the parent fiber sarcolemma through M-cadherin (Yin et al., 2013), but mSCs or their progeny may also interplay by direct contact or paracrine signals with a variety of neighboring supportive cells, including endothelial cells (ECs) (Christov et al., 2007), resident connective tissue cell types, such as poorly defined 'peri-endothelial' cells (Abou-Khalil et al., 2009) and $FCp4^+$ fibroblasts (Mathew et al., 2011; Murphy et al., 2011), and blood-borne macrophages (Arnold et al., 2007; Lescaudron et al., 1999; Lu et al., 2011; Sonnet et al., 2006).

At birth, muscle vascularization is rudimentary, with most growing myofibers being unconnected to capillaries during early post-natal development (Sallum et al., 2013), i.e. when mSCs actively proliferate to generate fusion-competent myoblasts for muscle growth (White et al., 2010). By contrast, in adult muscle, mSCs are closely associated to capillary vessels, and reside in a quiescent state in this vascular niche (Christov et al., 2007). The molecular and cellular mechanisms leading to the establishment of a functional vascular niche during development remain poorly defined. During embryonic stages, muscle patterning is governed by large vessel growth-promoting juxta-vascular connective tissue formation at the expense of muscle (Tozer et al., 2007). This progressively splits the initial bud into distinct muscle masses and explains the stereotyped organization of the muscle arterial tree with epimysial arteries feeding arcade arterioles running at the margin of each muscle fascicle (Bloch and Iberall, 1982; Gitiaux et al., 2013). Perimysial arcades produce transverse arterioles that penetrate at a right angle into the fascicle and fork four times before the terminal arteriole level, where six to eight capillaries are formed (Bloch and Iberall, 1982; Gitiaux et al., 2013).

In regenerating muscle, angiogenesis and myogenesis are spatiotemporally coordinated and appear to be regulated by common soluble factors (Christov et al., 2007) such as VEGFA (Williams and Annex, 2004), the master driver of sprouting angiogenesis (Coultas et al., 2005) that also stimulates myogenic cell growth (Chazaud et al., 2003; Christov et al., 2007). Sprouting angiogenesis takes place during late developmental stages and tissue repair (De Smet et al., 2009). In angiogenic sprouts, endothelial tip cells are the leading cells that (1) migrate in response to pro-angiogenic signals, (2) control adjacent ECs in a hierarchical manner to form stalk ECs that maintain connectivity with the parental vessel and (3) release PDGF-B to recruit $PDGFR^+$ pericytes to stabilize the endothelial tube (Armulik et al., 2011; De Smet et al., 2009).

This stabilizing effect is mediated by angiopoietin (ANGPT) 1 acting on the TIE2 receptor to induce EC quiescence, survival and strong cell-cell contacts (Armulik et al., 2011). This key signaling pathway for vascular homeostasis (Shim et al., 2007; Thomas and Augustin, 2009; Wakui et al., 2006) also applies to non-vascular cells (Valable et al., 2003). In particular, ANGPT1:TIE2 signaling regulates the hematopoietic stem cell quiescence (Arai et al., 2004).

[1]Institut Mondor de Recherche Biomédicale, INSERM U955-E10, Faculté de Médecine, 8 rue du Général Sarrail, Créteil F-94010, France. [2]Université Paris-Est, 5 boulevard Descartes, Marne-la-Vallée cedex 2 F-77454, France. [3]Université Paris-Est Créteil, 62 avenue du Général de Gaulle, Créteil F-94000, France. [4]Université d'Evry-Val d'Essonne, Boulevard François Mitterrand, Evry F-91000, France. [5]Etablissement Français du Sang, Créteil 94017, France. [6]Université Paris-Est, Ecole Nationale Vétérinaire d'Alfort, Maisons-Alfort 94700, France. [7]Hôpital Henri Mondor, Département de Pathologie, 51 avenue du Maréchal de Lattre de Tassigny, Créteil F-94010, France.
*These authors contributed equally to this work

‡Author for correspondence (romain.gherardi@hmn.aphp.fr)

Received 13 July 2014; Accepted 3 February 2015

Development (2015) 142, 1242-1253 doi:10.1242/dev.115386

In the same way, mSCs express the receptor TIE2 and respond to ANGPT1:TIE2 signaling, in terms of growth inhibition, pro-survival effects and self-renewal (Abou-Khalil et al., 2009). The exact sources of ANGPT1 that targets mSCs remain ill-defined.

Pericytes are mural cells embedded into the capillary basal lamina. There is no truly specific pericyte marker but pericytes typically express neuroglial 2 proteoglycan (NG2) (Ozerdem et al., 2001). They are detected at highly variable EC:pericyte ratios in different tissues, and are important for angiogenesis, microvasculature structural integrity and blood flow regulation (Armulik et al., 2011). Pericytes in skeletal muscle biology had been neglected until their recognition as mesenchymal stem cells with myogenic potential (Amos et al., 2008; Crisan et al., 2008; Dellavalle et al., 2007). Based on markers and morphology, pericytes are heterogeneous (Bondjers et al., 2006). In particular, muscle pericytes have been subtyped according to the expression of nestin, with type 1 nestin^{-}NG2^{+} pericytes, which are profibrotic and adipogenic, and type 2 nestin^{+}NG2^{+} pericytes, which have myogenic potential (Birbrair et al., 2013). The stem cell properties of pericytes may have potential therapeutic applications (Dellavalle et al., 2011; Morgan and Muntoni, 2007) and physiological relevance (Dellavalle et al., 2011). Here, we have investigated the role of pericytes in the mSC niche by analyzing their spatiotemporal and functional relationships with mSCs during muscle post-natal growth.

RESULTS

Post-natal angio-myogenesis

Temporal relationships between post-natal myogenesis and angiogenesis were analyzed on cross-sections of the gastrocnemius muscle of C57BL/6J mice, using immunostaining for PAX7 (mSCs), CD31/PECAM (ECs) and the proliferation marker KI67. The number of CD31^{+} capillaries increased from 8 to 100 per 100 myofibers from P1 to P31. At the same time, myofibers increased in size, their caliber growing from less than 10 µm to over 24 µm from P1-P9 to P15-P31 (Fig. 1A). Meanwhile PAX7^{+} mSCs dramatically decreased from 54 to 6 per 100 myofibers from P1 to P22-P31 (Fig. 1B). PAX7/KI67 double immunostaining showed a decrease in proliferating mSCs from more than 25 PAX7^{+}KI67^{+} cells per 100 myofibers at P1 to none at P31, demonstrating the progressive entry of mSCs into a generalized quiescent state (Fig. 1B).

To control the specificity of the NG2 marker in post-natal mouse skeletal muscle, we examined the immunohistochemical expression of NG2, laminin 1, CD34 and CD31 in adult TA and gastrocnemius muscles. NG2^{+} cells were almost always unequivocally identified as pericytes in capillaries and smooth muscle cells in arterioles. We never detected NG2^{+} expression in PAX7^{+} mSCs or in fibroblasts expressing CD34 and devoid of laminin 1^{+} basement membrane. No NG2^{+} cells co-expressed the CD31 EC marker. During post-natal microvascular growth into the endomysium, NG2^{+} cell coverage of ECs remained stable, with a mean of 78 pericyte nuclei per 100 EC nuclei from P1 to P16 (Fig. 1C). The ratio increased at P22 to the adult value of 90±8 per 100, assessing concurrent microvascular vascular growth arrest and maturation (Fig. 1C,D). Triple immunostaining for PDGFRβ/CD146/NG2 compared with single NG2 immunostaining produced similar quantitative results at P1, P3, P5, P8, P16, P22 and P60 (data not shown).

Spatial relationships between pericytes and mSCs were examined using NG2/PAX7 double immunostaining. During post-natal development, pericytes were initially remote from mSCs (Fig. 1E) with only 24% of PAX7^{+} mSCs being at less than 5 µm from a NG2^{+} cell (Fig. 1F). Then pericytes progressively entered in the close vicinity of a growing proportion of mSCs (Fig. 1E), reaching a plateau at the end of muscle microvascular growth with 73% of mSCs being found at less than 5 µm from a pericyte at P22 (Fig. 1F). Strikingly, this novel microvascular organization set up correlates with the progressive establishment of mSCs quiescence (Fig. 1B), and is in line with the non-random association between capillaries and adult mSCs (Christov et al., 2007). Taken together with myofiber growth and angiogenesis kinetics (Fig. 1A), these results indicate that during post-natal days, pericytes associated with growing microvessels are initially remote from actively cycling mSCs, and, as microvessels extend and mature, progressively enter in the mSC vicinity while mSCs either fuse with growing myofibers or become mitotically quiescent.

Progressive reduction of the distance between pericytes and mSCs was similarly observed in humans from 2 months of age to adulthood using double immunostaining for α smooth muscle actin (αSMA), a marker of human pericytes (Ozerdem et al., 2001), and CD56/NCAM, a marker of human mSCs (Fig. 1G). Confocal microscopy allowed 3D visualization of intimate proximity of NG2^{+} pericytes and CD56^{+} mSCs, allowing paracrine signaling (Fig. 1H). Triple immunostaining for NG2, CD56 and merosin/laminin 2, a myofiber basal lamina marker, did not detect conspicuous basal lamina interruption, allowing direct cell contacts in homeostatic muscle (Fig. 1I).

Pericyte subtyping was carried out using nestin immunostaining. Both nestin^{-} and nestin^{+} cells were found among NG2^{+} cells (Fig. 1J), but most adult PAX7^{+} mSCs were associated with nestin^{+} cells (Fig. 1K). Similar proportions of NG2^{+} (72%) and nestin^{+} (76%) cells found in the vicinity of mSCs confirmed that pericytes in mSC niche are type 2 pericytes (Birbrair et al., 2013). On these grounds, co-cultures under conditions avoiding cell-cell contacts and possible confusion with pericyte myogenic differentiation were used to characterize the functional influence of human microvascular cells on human mSC behavior.

The dual effect of pericytes on MPC behavior

Functional interactions between either ECs or pericytes with myogenic cells were first assessed using indirect co-cultures. Human mSC-derived myogenic progenitor cells (MPCs) were conventionally extracted after pronase digestion using anti-CD56-coupled magnetic beads, and plated at normal density (3000 cells/cm^{2}) in the lower chamber of culture wells, whereas the upper compartment, separated by a porous filter, was seeded with human umbilical vein ECs, human microvascular ECs or muscle pericytes. As previously reported (Christov et al., 2007), the two EC types induced strikingly similar increase in mSC-derived MPC growth (data not shown), and, therefore, human umbilical vein ECs were used and referred to as ECs in further experiments. Cells extracted from fresh human muscle tissue explants (Dellavalle et al., 2007), plated three or four times, and sorted as CD146^{+} and CD56^{-} using microbeads, were referred to as muscle pericytes as they expressed NG2, CD146, PDGFR and αSMA, as reported by Crisan et al. (2008), and were negative for CD45 (haematopoietic lineage cells), CD31 (ECs), CD56 (mSCs), desmin (skeletal and smooth muscle cells) and CD34 (fibroblasts and other interstitial cells).

ECs, compared with other MPCs used as controls, showed strong stimulatory effect on MPC growth in the lower chamber (+64% after 10 days of co-culture, $P<0.0001$) (Fig. 2A,B). By sharp contrast, pericytes significantly decreased MPC growth (−27%, $P<0.0001$). ECs increased the MPC fusion index in proportion to MPC density after 10 days of co-culture. By contrast, pericytes strongly stimulated myotube formation while decreasing MPC growth, suggesting a specific pro-differentiation effect (Fig. 2A,C). This

Development (2015) 142, 1242-1253 doi:10.1242/dev.115386

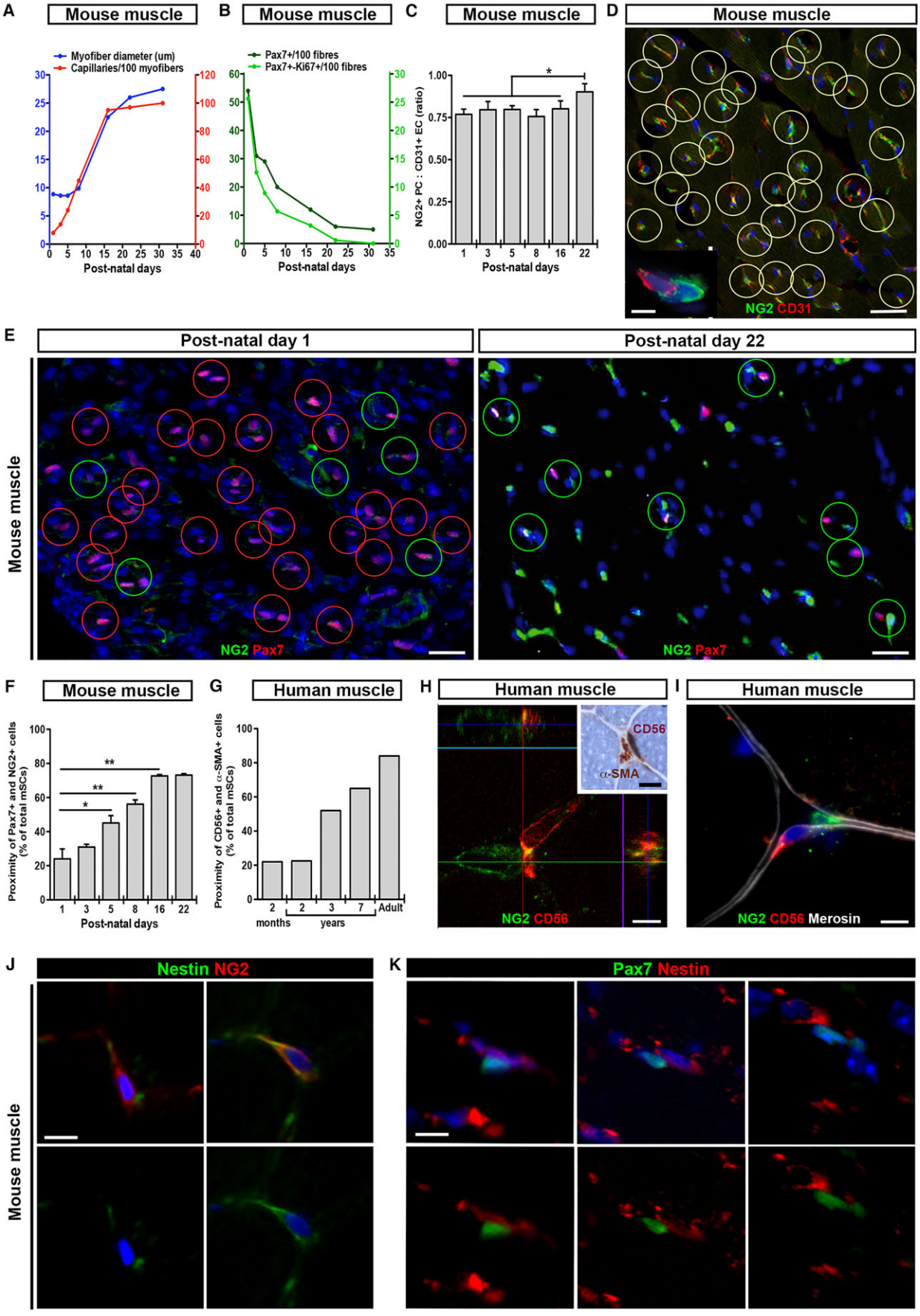

Fig. 1. See next page for legend.

Development (2015) 142, 1242-1253 doi:10.1242/dev.115386

Fig. 1. Spatiotemporal relationships between post-natal angiogenesis and myogenesis. (A) Post-natal increase in the myofiber diameter (blue line) and of the number of CD31$^+$ capillaries per 100 myofibers (red line) in mice. (B) Post-natal decrease in PAX7$^+$ mSCs (dark-green line) and of cycling PAX7$^+$KI67$^+$ mSCs (light-green line) per 100 myofibers. (C) NG2$^+$PC:CD31$^+$ EC ratio during post-natal mouse muscle development (PC, pericytes). Results are mean±s.e.m. (D) Pericyte coverage of adult mouse muscle capillaries. Yellow circles indicate CD31$^+$ EC (red) closely associated with NG2$^+$ pericytes (green). Scale bars: 10 µm; 2 µm in inset. (E) Increasing proximity of NG2$^+$ pericytes and PAX7$^+$ mSCs from P1 to P22 in mouse muscle. Red circles indicate mSCs remote from pericytes, green circles indicate mSCs at less than 5 µm from a pericyte. Scale bars: 10 µm. (F) Decreasing distance between pericytes and mSCs during post-natal development in mice. Results are mean±s.e.m. (G) Decreasing distance between pericytes and mSCs during post-natal development of human deltoid muscle. (H) Intimate proximity between pericytes (green) and mSCs (red) visualized in human muscle by confocal microscopy. Scale bar: 2 µm. Inset shows αSMA$^+$ pericyte (brown) and CD56$^+$ mSC (dark red). Scale bar: 5 µm. (I) The myofiber merosin$^+$ basal lamina (white) is interposed between pericytes (green) and mSCs (red) in human muscle. Scale bar: 5 µm. (J) Among NG2$^+$ pericytes (red), both nestin$^-$ and nestin$^+$ (green) pericytes are observed in the endomysium of mouse TA muscle. Scale bar: 5 µm. (K) Only type 2 nestin$^+$ pericytes (red) are tightly associated with PAX7$^+$ mSCs (green). Scale bar: 5 µm. *P<0.05, **P<0.01.

was supported by RT-qPCR, showing significant upregulation of the myogenic differentiation factors MYOD1 and myogenin (Fig. 2D). Notably, pericytes directly co-cultured with ECs in the upper chamber at a 2:3 ratio, which mimics the *in vivo* ratio during the post-natal period, had even stronger pro-differentiation effects on MPCs, as assessed by both the increased fusion index (Fig. 2A, C) and upregulation of MYOD1 and myogenin mRNAs (Fig. 2D). Thus, indirect co-cultures suggested that ECs may induce MPC growth, whereas pericytes may exert a dual effect, inhibiting growth and inducing MPC differentiation.

To uncouple potential cell density effect and differentiation, MPCs were cultured at low density (100 cells/cm^2) and exposed to EC- or pericyte-conditioned medium (CM) for 21 days. EC-CM increased MPC growth up to 4.3-fold at 4, 10 and 21 days of culture without a concurrent increase in the fusion index. By contrast, pericyte-CM increased MPC differentiation in myotubes by over fourfold at 4, 10 and 21 days of culture (Fig. 2E,F). These results were confirmed by myosin heavy chain staining (Fig. 2G).

Next, individual myofibers were cultured in human EC- or pericyte-CM, using floating conditions that preserve mSCs in their physiological environment beneath the basal lamina in contact with the myofiber (Pasut et al., 2013; Zammit et al., 2004). Mouse myofibers were used because whole myofibers cannot be isolated from human muscle, whereas human recombinant ANGPT1 has been efficiently used on isolated mouse myofibers (Abou-Khalil et al., 2009). Immunolabeling for PAX7 and MYOD1 showed that a 72 h exposure to EC-CM increased the proportion of activated PAX7$^+$/MYOD1$^+$ mSCs by 25% compared with controls cultured in unconditioned media (UCM). By contrast, pericyte-CM increased the proportion of mSCs at differentiation stage (PAX7$^-$/MYOD1$^+$) by 19%, at the expense of PAX7$^+$/MYOD1$^+$ cells that decreased by 25% compared with controls (Fig. 2H,I). In conclusion, ECs support proliferation of activated mSCs, and pericytes promote the differentiation program in a physiologically relevant culture system. The MPC fusion-inducing effect of pericytes was associated with maintenance of a pool of unfused mononucleated cells (Fig. 2A). To examine whether these cells could represent 'reserve cells' returned to a dormant state, we used pulse-chase experiments with 5-ethynyl-2′-deoxyuridine (EdU), a thymidine analog that is incorporated into the DNA of dividing cells (Fig. 3A). After a period of chase, the label dilutes in proportion to cell cycle activity: its retention at high concentration being characteristic of cells that have returned to quiescence (Chehrehasa et al., 2009). MPCs cultured in UCM for 4 days and subjected to an EdU pulse showed four levels of EdU label intensity after 2 h. After chases of 4 and 10 days, EdU dilution was observed and cells with very high labeling were not found (Fig. 3B,C). EC-CM induced more rapid EdU dilution compared with controls, with 71.8% and 84.9% of EdU^{Low} cells at 4 and 10 days of culture, respectively (Fig. 3C). By contrast, exposure to pericyte-CM was associated to conspicuous EdU retention, with decrease of both EdU^{Low} cells (7.2% at 4 days; 11.9% at 10 days) and EdU^{Intermediate} cells (24.1% at 4 days; 26.4% at 10 days), and marked increase of both EdU^{High} cells (37.8% at 4 days; 30.9% at 10 days) and EdU$^{Very\ high}$ cells (36% at 4 days; 25.7% at 10 days) (Fig. 3C). These results assessed EC-induced mitogenic effect and pericyte-induced cycle arrest.

To examine whether MPC cycle arrest was related to quiescence or to differentiation, EdU detection after 10 days was coupled with various immunostainings: EdU^{High} and EdU$^{Very\ high}$ cells expressed PAX7 (82.8%) but only a small minority expressed proliferation and differentiation markers (11.6% KI67$^+$, 18.4% MYOD1$^+$ and 13.2% myogenin$^+$ MPCs), indicating that pericyte-induced EdU-retaining cells were mostly reserve cells (Fig. 3D). In summary, in addition to promoting myotube formation, pericytes induce MPC quiescence.

ANGPT1 and IGF1 as pericyte effectors

To detect secreted factors that may mediate EC and pericyte effects on mSCs, 121 cytokines and growth factors were screened by ELISA on 48 h culture supernatants. Compared with UCM, pericyte-CM showed increases in 14 molecules (ANGPT1, TGFβ1, PIGF, IGF1, HGF, MCP1, GRO, angiogenin, MIF, SGP130, TIMP1, uPAR, VEGFA and osteoprotegerin) and EC-CM showed increases in 18 molecules (ANGPT2, PDGF-BB, TGFβ1, TGFβ2, FGF6, EGF, BMP4, MCP1, GRO, angiogenin, IL8, IL1R4/ST2, I-TAC, MIF, SGP130, sRNF RII, TRAIL R3 and uPAR). Several of these factors have previously been shown to exert different effects on myogenic cells. Vascular cell factors with the highest cognate receptor expression by human MPCs were identified using mRNA profiling of 84 receptor genes. Pericyte-CM contained only two factors with receptors highly expressed by MPCs (Table 1): IGF1, a key factor in muscle differentiation and growth (Duan et al., 2010); and ANGPT1, a factor that promotes stem cell quiescence (Abou-Khalil et al., 2009). These factors remained similarly secreted when pericytes were co-cultured with ECs at a 2:3 ratio to mimic the *in vivo* situation (data not shown). In EC-CM, ANGPT1 and IGF1 were, respectively, undetectable and not significantly increased compared with UCM (Table 1).

Whole-genome transcript analysis of mSCs performed after GFP-based FACS sorting from muscle of PAX3$^{GFP/+}$ mice showed that mSCs differentially express receptors of the pericyte products during post-natal development (Fig. 4A-D). Consistent with progressive post-natal mSC entry in quiescence, transcription of IGFR1 and the downstream insulin signaling pathway factors involved in protein synthesis decreased progressively from post-natal P1 to P28, whereas TIE2 transcription progressively increased together with the downstream MAPK pathway molecules previously shown to mediate ANGPT1:TIE2 pro-quiescence effects on MPCs (Abou-Khalil et al., 2009).

Functional involvement of pericyte-released IGF1 and ANGPT1 was analyzed and compared with the two EC factors with the highest level of constitutive expression of cognate receptors in mSCs (Table 1), including ANGPT2, a natural ANGPT1 antagonist that

Development (2015) 142, 1242-1253 doi:10.1242/dev.115386

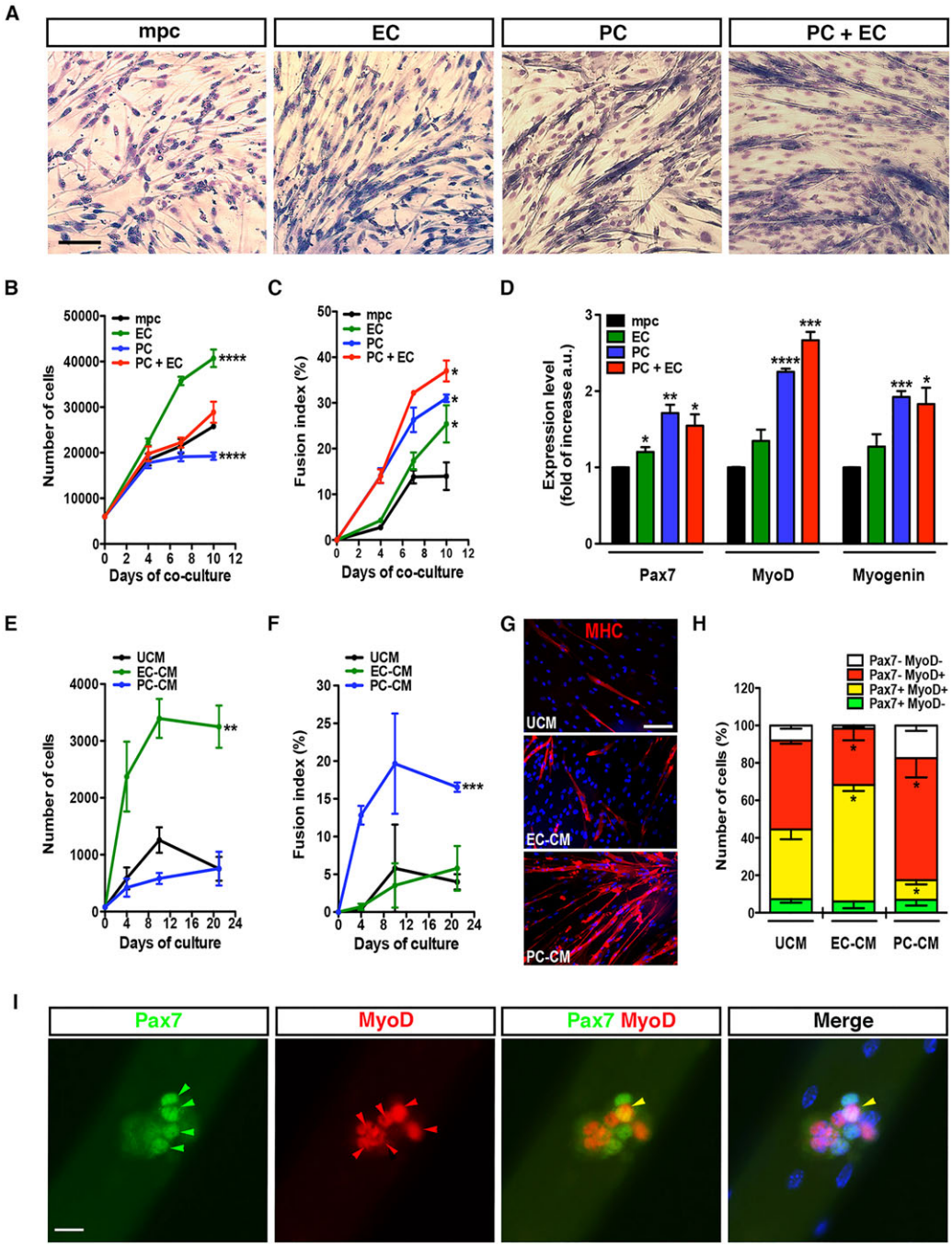

Fig. 2. Opposing *in vitro* effects of pericytes and ECs on MPCs. (A-D) MPCs co-cultured in transwells with other MPCs, ECs, pericytes (PCs) or ECs+PCs for 10 days. (A) MPCs in lower wells show increased growth in the presence of upper insert ECs and increased myotube formation in presence of upper insert PCs or PCs+ECs. (B) MPC growth curves. (C) Fusion index curves. (D) RT-qPCR on lower well MPCs after 10 days of co-culture, showing upregulation of PAX7 in the presence of ECs, and of PAX7, MYOD1 and myogenin in presence of PCs or PCs+ECs. Results are mean±s.e.m. (E,F) MPCs cultured at low density in conditioned media (CM) for 21 days, showing growth effect of EC-CM (E) and differentiation effect of PC-CM (F) compared with unconditioned medium (UCM). Results are mean±s.e.m. (G) Myosin heavy chain (MHC) immunostaining with nuclear counterstaining distinctly shows increased numbers of mononucleated cells in EC-CM and increased MHC^{+} myotubes in PC-CM, compared with UCM. (H,I) Isolated myofibers cultured in CM for 72 h and stained for PAX7 (green) and MYOD1 (red). EC-CM increases the percentage of activated of PAX7^{+}/MYOD1^{+} MPCs, whereas PC-CM increases MPC differentiation (PAX7^{-}/MYOD1^{+}) compared with UCM (H). Representative picture of PAX7/MYOD1 labeling (I). Results are mean±s.e.m. Arrowheads in I indicate PAX7^{+} (green), MYOD1^{+} (red) and double-stained cells (yellow) (769 mSCs analyzed on 22 myofibers in UCM, 760 on 13 in EC-CM and 865 on 18 in PC-CM. Scale bars: 10 µm in A; 20 µm in G; 5 µm in I. *P<0.05, **P<0.01, ***P<0.001, ****P<0.0001.

competitively binds TIE2 (Maisonpierre et al., 1997), and PDGF-BB, a mitogenic factor for cells of mesenchymal origin previously shown to stimulate MPC proliferation (Christov et al., 2007). This was achieved by adding blocking agents at saturating conditions to conditioned media added to MPC cultures every 2 days, including specific blocking antibodies against IGF1, PDGF-BB and the TIE2Fc fragment, to block pericyte-released ANGPT1 or EC-released ANGPT2 (Fig. 4E-G). After 10 days, non-significant change was observed in terms of growth, EdU retention and differentiation when human MPCs were grown at normal density in

Development (2015) 142, 1242-1253 doi:10.1242/dev.115386

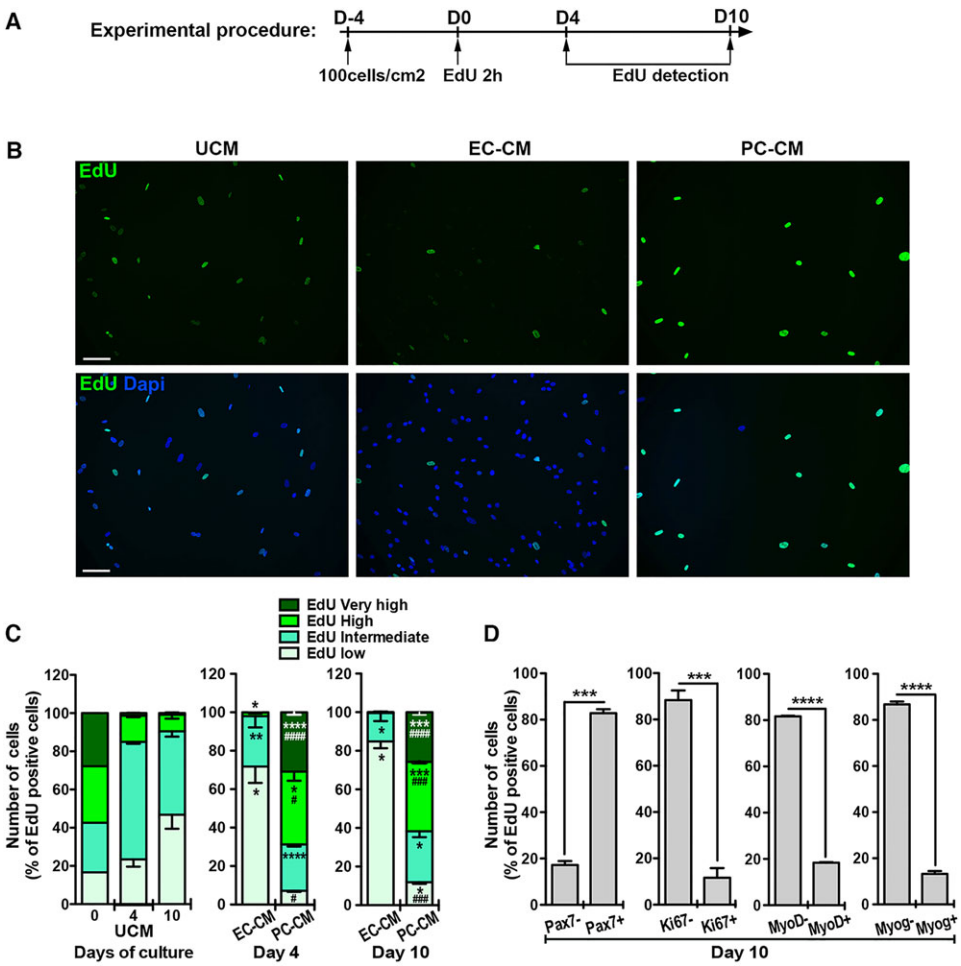

Fig. 3. Opposing *in vitro* effects of pericytes and ECs on MPC EdU retention. (A) Experimental EdU pulse/chase procedure. (B) EdU MPC labeling after 10 days of MPC culture at low density showing decreased EdU retention in EC-CM and increased EdU retention in PC-CM. Scale bars: 20 µm. (C) Relative proportions of MPCs with low to very high EdU retention confirm EdU dilution in EC-CM and increased EdU retention in PC-CM compared with UCM at both 4 and 10 days of culture. Results are mean±s.e.m. Significant differences are indicated by * (comparison with UCM) and by # (EC-CM versus PC-CM). (D) Most MPCs showing high or very high EdU retention expressed PAX7 but not KI67, MYOD1, and myogenin, as expected for reserve cells (n=4 per group, results are mean±s.e.m.). * or $^{\#}P$<0.05, *** or $^{\#\#\#}P$<0.001, **** or $^{\#\#\#\#}P$<0.0001.

the presence of UCM incubated with the blocking agents, polyclonal IgG or non-specific antibody. By contrast, addition of anti-IGF1 antibody markedly reversed the differentiating effects of pericyte-CM (Fig. 4E); anti-PDGF-BB antibody added to EC-CM significantly decreased MPC growth (Fig. 4F), as previously reported (Christov et al., 2007). TIE2Fc treatment significantly reduced pericyte-induced MPC EdU retention (Fig. 4G). As PC-CM contained tenfold more ANGPT1 than ANGPT2, and no effect was observed in UCM conditions despite similar amounts of ANGPT2, it is likely that the TIE2Fc effect in PC-CM reflected blockade of ANGPT1-induced MPC quiescence. By contrast, EC-CM contained high levels of ANGPT2. As expected from blockade of the ANGPT2 antagonistic action on MPC autocrine ANGPT1:TIE2 signaling (Abou-Khalil et al., 2009), TIE2Fc reduced EC-induced MPC EdU dilution, notably restoring the $EdU^{Very\ high}$ MPC pool to control values (Fig. 4G). Consistent with this, MPC growth increased upon blockade of ANGPT1 in pericyte-CM and decreased upon blockade of ANGPT2 prominently detected in EC-CM.

Table 1. Candidate effectors released by pericytes and ECs, and MPC expression of cognate receptors

Secreted proteins with cognate receptors on MPC‡				Receptors expressed by MPC	
	UCM	PC-CM	EC-CM		
Name	Mean intensity			Name	Intensity (>100)
IGF1	691	978**	838	IGFR1	189
ANGPT1	0	8000****	0	TIE2	208
ANGPT2	571	669	8014****		
PDGF-BB	140	226	11,028****	PDGFRβ	221
				PDGFRα	450
TGFβ1	306	381*	475**	TGFβR3	122
TGFβ2	76	89	112*		
FGF6	249	288	326*	FGFR1	193

*P<0.05, **P<0.01, ****P<0.0001.
‡Three primary cultures per condition analyzed in duplicate.

Post-natal ablation of muscle pericytes

The relevance of these elementary findings to post-natal muscle growth was assessed by lineage tracing and specific cell ablation using a pericyte-specific Cre/LoxP system. As NG2 is exclusively expressed by mural cells during vascular morphogenesis (Ozerdem et al., 2001), we first used a *NG2-Cre* mouse [*B6;FVB-Tg(Cspg4-cre)1Akik/J*-Jax]. Cre efficiency was assessed by crossing *NG2-Cre* with *R26-Flox-STOP-lacZ* reporter (*R26R*) mice. In TA muscle of adult $Tg{:}NG2^{Cre/+}{::}R26R^{lacZ}$ mice, 14% of $NG2^{+}$ cells strongly expressed β-gal in their cytoplasm (Fig. 5A). Only 0.7% of myofibers expressed β-gal, which was inconsistent with NG2 transcription in muscle cells during development. mSCs were examined on isolated myofibers immediately (n=233, three mice) or after 72 h of culture in high-activation medium (n=132, three mice). At t0, 972 mSCs were counted, of which 2.44% expressed β-gal. After 3 days in high-activation medium, 1584 clusters of mSC daughter cells were found, including 9.38±3.52 cells per cluster: 3% of clusters were entirely $\beta\text{-gal}^{+}$; only 1.7% showed mixture of $\beta\text{-gal}^{+}$ and $\beta\text{-gal}^{-}$ cells; and 95.3% were totally $\beta\text{-gal}^{-}$, ruling out significant reporter gene expression inherent to myoblast activation. Thus, the very small

Development (2015) 142, 1242-1253 doi:10.1242/dev.115386

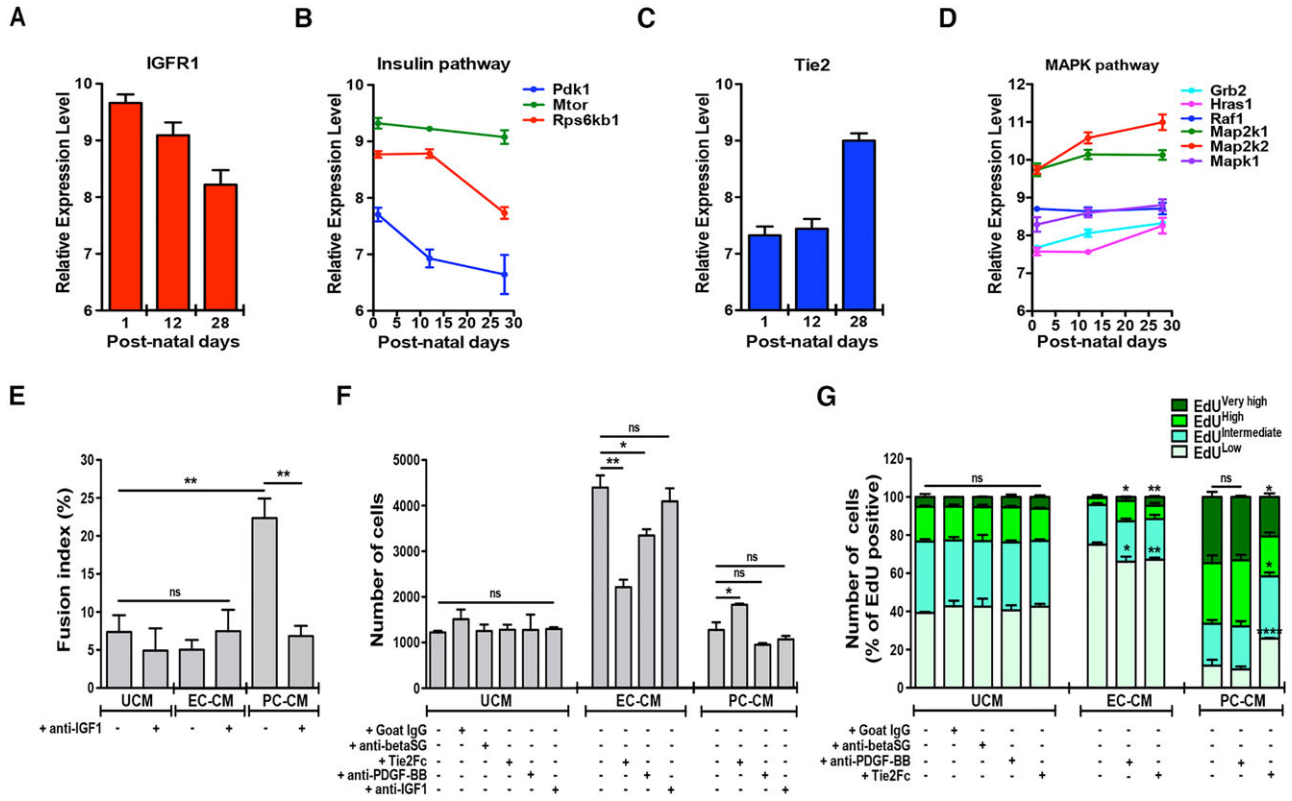

Fig. 4. Pericyte and EC effectors. (A,B) As assessed by whole-genome transcript analysis of mSCs performed after GFP-based FACS sorting from the muscle of PAX3$^{GFP/+}$ mice, IGFR1 gene transcription tended to decrease from post-natal day P1 to P28, a time period during which the bulk of extracted mSCs are successively in their proliferation, differentiation and quiescence states. Transcription of the downstream insulin signaling pathway factors involved in protein synthesis also decreased at P28. (C,D) In the same analysis, as opposed to IGFR1, TIE2 gene transcription increased from P1 to P12 and from P12 to P28, together with that of the downstream MAPK pathway molecules involved in ANGPT1:TIE2-mediated pro-quiescence effects. (A-D) Arbitrary units correspond to Affymetrix array fluorescence intensity levels. Error bars represent s.e.m. of three repeated analyses of a single sample. (E) *In vitro* IGF1 inhibition produced by blocking antibody reverses PC-CM effect on MPC fusion index, i.e. the pericyte pro-differentiation effect. (F) Both ANGPT2 inhibition by TIE2Fc and PDGF-BB inhibition by blocking antibody decreased EC-CM-induced MPC growth effect. By contrast, the ANGPT inhibitor TIE2Fc increased MPC growth in PC-CM, a CM strongly enriched in ANGPT1. (G) EdU retention by MPCs grown in CM varied upon effector signaling blockade, consistent with EC or pericyte effects on MPC growth and quiescence, respectively. (E-G) n=3 cultures per condition, results are mean±s.e.m. *P<0.05, **P<0.01, ****P<0.0001.

proportion of β-gal$^+$ myofibers illustrated in Fig. 5A likely corresponds to the marginal contribution made by pericytes to post-natal myogenesis [estimated at 0.4-0.6% of myofibers in TA muscle by Dellavalle et al. (2011)]. The negligible proportion of non-vascular cells expressing NG2-Cre in TA muscle led us to cross the *NG2-Cre* mouse with the *Cre-inducible Flox-STOP-diphtheria toxin* (*DT*) *receptor* (*iDTR*) mouse, to obtain a model for selective DT-induced depletion of NG2$^+$ pericytes and vascular smooth muscle cells. After 48 h of DT injection in TA muscle, adult *Tg:NG2$^{Cre/+}$::R26R^{iDTR}* mice showed a similarly low number of necrotic myofibers (<2.7%) compared with littermate controls, conspicuous pericyte loss [31 versus 57 (−46%) NG2$^+$ cells per 100 myofibers] and mSC increase (4.3 versus 3 PAX7$^+$ cells per 100 myofibers). DT was injected into the growing TA muscle of *Tg:NG2$^{Cre/+}$::R26R^{iDTR}* mice at P13 (Fig. 5B). Eight days later, the injected muscle appeared reduced in size compared with the contralateral TA muscle (Fig. 5C). Compared with littermate controls injected with DT, *Tg:NG2$^{Cre/+}$::R26R^{iDTR}* mice showed a conspicuous decrease of NG2$^+$ pericytes (−29.5%) (Fig. 5D). The small number of myofibers with internal nuclei (due to post-injury regeneration) (0.55-2.20% in *Tg:NG2$^{Cre/+}$::R26R^{iDTR}* mice versus 0.51-1.48% in littermates) were excluded from morphometric evaluation. Pericyte depletion was associated with significant myofiber hypotrophy (16.3±0.6 versus 18.3±0.6 µm, P<0.05) (Fig. 5E), with a mild increase in total of PAX7$^+$ mSCs (16.7%) and marked increase of cycling PAX7$^+$KI67$^+$ mSCs (+202%) (Fig. 5F). Of note, the amount of pericyte ablation in *Tg:NG2$^{cre/+}$::R26R^{iDTR}* mice was higher than predicted by *lacZ* reporter gene expression, and, in addition, it differed in adult and pup experiments. The non-linear relationship between X-gal staining intensity and the level of recombination has been previously documented in different muscle areas, and attributed to differences in activity of the ROSA26 promoter or to the stability of β-gal protein across different muscle areas (McCarthy et al., 2012). Minor iDTR expression at the cell surface may be sufficient to confer sensitivity to DT, whereas minute amounts of β-gal diluted into the cytosol may not be detectable microscopically. The somewhat lower extent of pericyte ablation observed after 8 days in the context of post-natal angiogenesis, compared with adult muscle examined 2 days after DT injection, was likely due to replenishment of emptied pericyte niches by novel cells expressing NG2, as previously reported (Rajantie et al., 2004). Our results therefore show that *in vivo* ablation of pericytes leads to mSC relief from quiescence.

Selective suppression of pericyte factors

We next used tissue-specific mouse mutants to characterize the role of the previously identified candidate pericyte effectors. We first crossed *NG2-Cre* mice with *Flox-IGF1* mice to selectively suppress

Development (2015) 142, 1242-1253 doi:10.1242/dev.115386

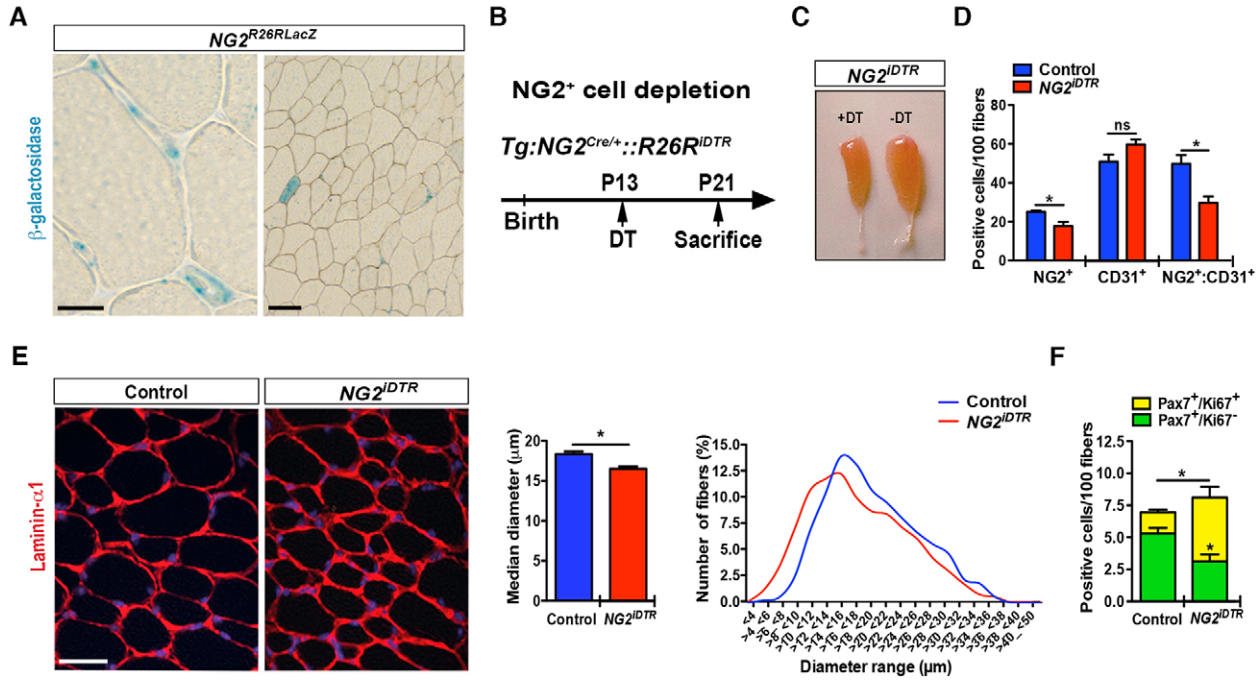

Fig. 5. *In vivo* muscle pericyte ablation effects on post-natal muscle growth and mSC behavior. (A) β-Gal expression in the TA muscle of *Tg:NG2*$^{Cre/+}$*::R26R*^{lacZ} mice: β-gal is selectively expressed in pericytes and microvascular smooth muscle cells, with >99% of β-gal^{-} myofibers. Scale bars: 5 µm (left); 30 µm (right). (B) Procedure for post-natal DT-induced muscle pericyte ablation in *Tg:NG2*$^{Cre/+}$*::R26R*^{iDTR} mice. DT is injected into muscle. (C) Hypotrophy of the DT-injected TA muscle (+DT) depleted in pericytes compared with contralateral TA muscle (–DT), 9 days after DT injection in *Tg:NG2*$^{Cre/+}$*::R26R*$^{iDTR/+}$ mice. (D) Muscle pericyte number decreased in the DT-injected muscle in *Tg:NG2*$^{Cre/+}$*::R26R*$^{iDTR/+}$ mice compared with littermate *Tg:NG2*$^{+/+}$*::R26R*$^{iDTR/+}$ controls (n=3 per group, results are mean±s.e.m.). (E) Myofibers were hypotrophic 9 days after DT injection in *Tg:NG2*$^{Cre/+}$*::R26R*$^{iDTR/+}$ mice compared with littermate *Tg:NG2*$^{+/+}$*::R26R*$^{iDTR/+}$ controls, as assessed by laminin 1α immunohistochemistry. Scale bar: 20 µm. Graphs show size distribution curves and mean myofiber diameter. Myonuclei of hypotrophic myofibers are peripherally located (n=4 per group, results are mean±s.e.m.). (F) Pericyte ablation in *Tg:NG2*$^{Cre/+}$*::R26R*$^{iDTR/+}$ mice compared with DT-injected littermate *Tg:NG2*$^{+/+}$*::R26R*$^{iDTR/+}$ controls is associated with increased net number of PAX7^{+} mSCs and increased proliferation assessed by KI67 expression (n=4 per group, results are mean±s.e.m.). *P<0.05.

pericyte IGF1 production. At post-natal day P21 (Fig. 6A), mice with *Igf1* gene deletion in pericytes compared with their littermates showed a decrease in total body weight (7-8%), TA muscle size, myofiber size (33.08±0.8 versus 29.08±0.7 µm, P=0.0002) (Fig. 6B,C) and number of myonuclei per myofiber (1.48±0.09 versus 2.14±0.09, P<0.0001) (Fig. 6D), supporting decreased mSC fusion as a mechanism of fiber hypotrophy.

ANGPT1 is a major pericyte factor involved in vascular development. To avoid lethality linked to lack of ANGPT1 at pre-natal stages (Jeansson et al., 2011), we looked for an inducible model to assess post-natal effects of ANGPT1 on mSCs. We took advantage of the previously characterized *Tissue Nonspecific Alkaline Phosphatase* (*TNAP*) *CreERT2* mouse, in which both NG2^{+} pericytes and CD31^{+} ECs, at a ratio of about 1:1, but not mSCs, express the TNAP-Cre (Dellavalle et al., 2011) (Fig. 6E). Because ANGPT1 is secreted by pericytes but not by ECs (Table 1), we crossed *TNAP CreERT2* and *Flox-Angpt1* mice to generate a model to conditionally suppress pericyte-derived ANGPT1. A series of three daily subcutaneous tamoxifen injections were given at P9, P10 and P11 in *Tg:TNAP*$^{CreERT2/+}$*::Angpt1*$^{del/+}$ mice and littermate controls (Fig. 6F). Similar to wild-type mice (Fig. 1B), control mice showed a 45.9% decrease of PAX7^{+} mSCs from P18 to P28 (10.2±1.1 versus 5.5±0.1 per 100 myofibers; P=0.0003). By sharp contrast, during the same time, *Tg:TNAP*$^{CreERT2/+}$*::Angpt1*$^{del/+}$ mice showed a 25% increase in PAX7^{+} mSCs. This was associated with dramatic increase in the proportion of PAX7^{+}KI67^{+} cycling mSCs, from 12.3±1 to 65.3±3.9% (Fig. 6G). The maximum mSC release from quiescence was observed at the time point (P28) associated with the highest expression of TIE2 in mSCs (Fig. 4C). This occurred in the absence of myofiber necrosis, and without concurrent changes in NG2^{+} pericyte and CD31^{+} EC numbers and myofiber size. Together with *in vitro* experiments, these results demonstrate that pericytes stimulate myofiber growth through IGF1 and control mSC quiescence through ANGPT1.

DISCUSSION

We show that post-natal angiogenesis is spatio-temporally coordinated with myofiber growth and with mSC entry in quiescence. During angiogenesis, pericytes control EC proliferation and survival (Franco et al., 2011), and basement membrane assembly (Stratman et al., 2009). In addition, pericytes, which are present in the niche of 70-80% of adult mSCs, significantly influenced myogenic cell behavior, through differentiation/growth-promoting effects of IGF1 and quiescence-promoting effects of ANGPT1. Notably, the high pericyte:EC ratio found in adult muscle by far exceeds classical electron microscopy-based estimations (Shepro and Morel, 1993). In contrast to pericytes, ECs were mitogenic for MPCs through ANGPT2 and PDGF-BB, and probably other growth factors (Christov et al., 2007). This indicates that different cell constituents within a stem cell niche exert distinct functions, and suggests fine-tuning of mSC behavior control by microvascular cells during post-natal growth.

The mSC microvascular niche comprises NG2^{+}nestin^{+} pericytes. Pro-quiescence effects of pericyte ANGPT1 on mSCs were assessed *in vitro* and *in vivo*, using the

Development (2015) 142, 1242-1253 doi:10.1242/dev.115386

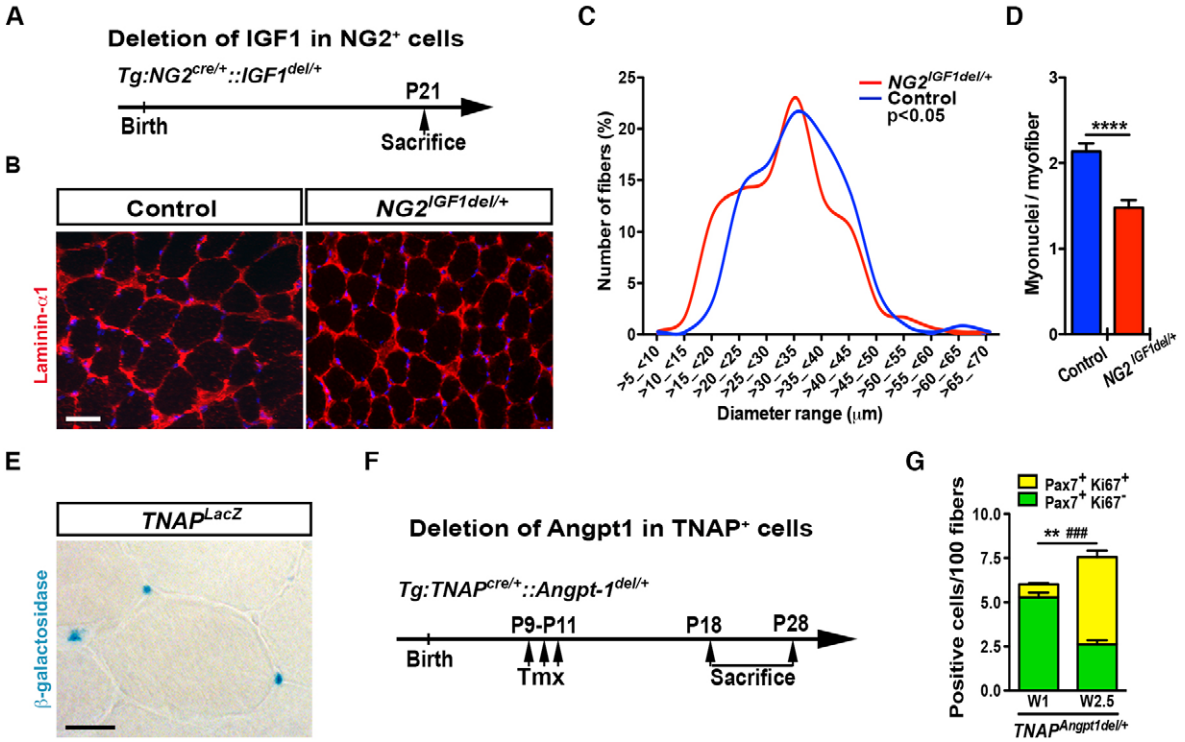

Fig. 6. Post-natal *Igf1* or *Angpt1* gene deletion in pericytes. (A) Procedure for *Igf1* gene deletion in *Tg:NG2*$^{Cre/+}$*::IGF1*$^{del/+}$ mice. (B-D) Pericyte IGF1 deletion in *Tg:NG2*$^{Cre/+}$*::IGF1*$^{del/+}$ mice resulted in myofiber hypotrophy (B,C) and decreased number of myonuclei per myofiber (D) compared with *Tg:NG2*$^{+/+}$*::IGF1*$^{del/+}$ littermate controls. *n*=3 mice per test. Results are mean±s.e.m. Scale bar: 20 µm. (E) Capillary cells selectively expressed β-gal in TA muscle of *Tg:TNAP*$^{CreERT2/+}$*::R26R*^{lacZ} mice. (F) Procedure for pericyte *Angpt1* gene deletion in *Tg:TNAP*$^{CreERT2/+}$*::Angpt1*$^{del/+}$ mice. (G) Selective post-natal heterozygous deletion of *Angpt1* gene in pericytes of *Tg:TNAP*$^{CreERT2/+}$*::Angpt1*$^{del/+}$ mice was associated with increased mSCs from P18 (three mice) to P28 (four mice), including net increase of PAX7^{+} cell net number and increase of cycling PAX7^{+}KI67^{+} mSCs. Results are mean±s.e.m. $^{**}P$<0.01, $^{\#\#\#}P$<0.001, $^{****}P$<0.0001.

Tg:TNAP$^{CreERT2/+}$ mouse model. Interestingly, lineage studies based on the same mouse model previously showed that TNAP^{+} pericytes have myogenic potential (Dellavalle et al., 2011), and, consistently, type 2 NG2^{+}nestin^{+} pericytes detected in the mSC microvascular niche were previously characterized as mesenchymal stem cells with prominent myogenic potential (Birbrair et al., 2013). Taken together, these data strongly suggest that ‘stem cells support other stem cells’ in skeletal muscle (Leatherman, 2013). In at least three different adult stem cell niches – the *Drosophila* testis, the hair follicle and the bone marrow stem cell niches – two separate populations of stem cells have been identified, with one cell type producing factors that contribute to the maintenance of the other one (Leatherman, 2013; Méndez-Ferrer et al., 2010). Consistent with our study, supportive cells in the hematopoietic stem cell niche have been characterized as NG2^{+}nestin^{+} smooth muscle vascular cells (Kunisaki et al., 2013).

Our results may be of practical interest as mesenchymal stem cells are increasingly used for therapeutic purposes and most functional benefits of these therapies have been linked to ill-defined trophic effects on existing tissue cells rather than to the expected differentiation of the grafted cells. We showed that pericyte-released IGF1 and ANGPT1, acting on adjacent muscle stem cells, may exert tight regulation of their post-natal fate, but the signals that may orient pericytes towards myogenic cell differentiation or a purely supportive action are unknown. To what extent pericytes may be instrumental in adaptive responses to disruption of local homeostasis, systemic signals and aging also remains to be delineated (Rojas-Ríos and González-Reyes, 2014).

MATERIALS AND METHODS

Patients

Normal deltoid muscle samples from 18- to 60-year-old patients were used to obtain human mSCs or pericytes. Normal deltoid muscle biopsies from patients aged from 2 months to 21 years were used to establish post-natal evolution of the spatial relationships between pericytes and mSCs. In accordance with the Henri Mondor hospital research ethics committee, all adult patients or the parents of patients under 18 years of age gave written informed consent for participation in the study.

Mice

B6;FVB-Tg(Cspg4-cre)1Akik/J (Zhu et al., 2008), C57BL/6-Gt(ROSA)26Sortm1(HBEGF)Awai/J (Buch et al., 2005), B6.129(FVB)Igf1tm1Dlr/J (Liu et al., 1998), B6.129S4-Gt(ROSA)26Sortm1Sor/J (Soriano, 1999) (Jax Mice), Angpt1tm1.1Seq (Jeansson et al., 2011) (a gift from Susan E. Quaggin, Northwestern University, Evanston, IL, USA), Tg(Alpl-cre/ERT2)12Gcos (Dellavalle et al., 2011) (a gift from G. Cossu, UCL, London, UK and A. Dellavalle, InScientiaFides, San Marino Republic) and C57BL/6J were bred and crossed in our facilities. The *Tg:NG2*$^{Cre/+}$*::R26R*^{iDTR}, *Tg:NG2*$^{Cre/+}$*::IGF1*$^{del/+}$ and *Tg:NG2*$^{Cre/+}$*::R26R*^{lacZ} mice were generated by crossing NG2-Cre either with *R26RDTR*$^{loxP/loxP}$ or *R26RlacZ*$^{stoploxP/stoploxP}$ animals, with PCR assessment of both transgenes. The *Tg:TNAP*$^{CreERT2/+}$*::Angpt1*$^{del/+}$ was generated by crossing TNAP-CreERT2 with *Angpt1*$^{loxP/loxP}$ animals with assessment by PCR for both transgenes. Genotyping strategies have been published for TNAP-CreERT2 (Dellavalle et al., 2011) and *Angpt1*$^{loxP/loxP}$ (Jeansson et al., 2011), and were supplied by Jax Mice for NG2-Cre, *R26RDTR*$^{stoploxP/stoploxP}$, *R26RlacZ*$^{stoploxP/stoploxP}$ and *Igf1*$^{loxP/loxP}$. The French Ethical Committee approved animal experiments (license number 11-00010).

In vivo procedures

For pericyte depletion, adult or P13 mice were injected in the TA muscle with DT (D0564; Sigma-Aldrich) diluted in physiological serum at 1 ng/g

Development (2015) 142, 1242-1253 doi:10.1242/dev.115386

body weight in adult mice (10 µl/TA) and at 3 ng/g in young mice (2 µl/TA). Contralateral muscle was injected with an equal volume of serum. Mice were sacrificed 8, 24 and 48 h after injection (adult mice), and at P21 (young mice). For *Angpt1* gene deletion, young mice were injected subcutaneously (50 µl) with 0.25 mg tamoxifen (T5648-1G; Sigma-Aldrich) diluted in corn oil (C8267; Sigma-Aldrich) at P9, P10 and P11, and sacrificed at P18 and P28.

Human cell cultures

All cell types were cultured at 37°C with 5% CO_2. To obtain MPCs, human mSCs were extracted from deltoid muscle samples after digestion by Pronase E (P5147; Sigma-Aldrich) at 1.5 mg/ml. After a few days of amplification, MPCs were purified using NCAM/CD56 microbeads according to the kit protocol (130-050-401; Miltenyi Biotec) and amplified in HAM F-12 medium (31765027; Life Technologies) supplemented with 20% fetal calf serum (FCS) (S1810-500; Dominique Dutscher), 1% penicillin/streptomycin (P/S; 15140122; Life Technologies), 0.2% MEM vitamins solution (11120037; Life Technologies), 2 mM non-essential amino acids (1114003; Life Technologies) and 1% Ultroser G serum substitute (15950-017; Pall Corporation).

Pericytes were extracted by explant from deltoid muscle samples (Tonlorenzi et al., 2007). After 2 weeks of culture, pericytes were purified using CD56 and CD146 microbeads (130-050-401 and 130-093-596; Miltenyi Biotec) and then amplified in M5 medium before use (Tonlorenzi et al., 2007). Purity was >98%, as assessed by both positive ($CD146^+NG2^+\alpha SMA^+$) and negative markers ($CD45^-CD31^-CD34^-desmin^-$).

Both human umbilical vein endothelial cells (C-12203; PromoCell) and human microvascular endothelial cells (C-12210; PromoCell) were cultured in endothelial cells basal medium (ECBM; C22010; PromoCell) supplemented with endothelial cell growth medium supplement mix (C-39215; PromoCell). In some experiments, ECBM supplemented with 2% FCS and 1% P/S was called unconditioned medium (UCM) and used to prepare 48 h culture-conditioned media of EC (EC-CM) or pericyte (PC-CM).

In transwell co-cultures, all cell types were grown in UCM renewed every 2 days. For 10 days, MPCs (3000 cells/cm^2) in the lower well were co-cultivated with control MPCs (67,000 cells/cm^2), pericytes (67,000 cells/cm^2), ECs (100,000 cells/cm^2) or pericytes+ECs (67,000+100,000 cells/cm^2) (upper insert reference: 353095; BD Falcon), then used for RT-qPCR or stained by May Grunwald Giemsa to assess MPC growth and differentiation. In low-density cultures, MPCs (100 cells/cm^2) were incubated with EdU (Click-iT EdU Alexa Fluor 488 Imaging Kit; C10337; Invitrogen) for 2 h and then cultured for 4, 10 or 21 days in the different CM renewed every 2 days (Chehrehasa et al., 2009).

Floating myofibers

Single myofibers were isolated from C57BL/6J EDL or $Tg{:}NG2^{Cre/+}{::}R26R^{lacZ}$ TA muscles (Beauchamp et al., 2000; Rosenblatt et al., 1995). Individual intact myofibers were incubated with UCM, pericytes-CM or EC-CM mixed (vol/vol) with low-activation medium [10% horse serum; 26050088; Life Technologies), 0.5% chicken embryo extract (CE-650-J; Seralab) and DMEM (11965092; Life Technologies)]. After 72 h of incubation, myofibers were used for PAX7/MYOD1 immunostaining as previously described (Guardiola et al., 2012; Zammit et al., 2004). The myofibers isolated from $Tg{:}NG2^{Cre/+}{::}R26R^{lacZ}$ TA muscle were stained with X-gal just after extraction or after 72 h of culture in high-activation medium (20% FCS, 1% chicken embryo extract and DMEM).

X-gal staining

Muscle sections or single myofibers were fixed in 0.2% glutaraldehyde for 5 min at room temperature, washed and then incubated overnight at 37°C in X-gal solution [400 µg/ml of X-gal (B4252; Sigma-Aldrich), 0.02% of Tween-20 (P9416; Sigma-Aldrich), 2 mM of $MgCl_2$ (Y02016; Life Technologies), 4 mM of potassium ferricyanide (26810.232; Prolabo), 4 mM of potassium ferrocyanide (P9387; Sigma-Aldrich) in PBS (14190094; Life Technologies)]. After incubation, muscle sections were mounted using Eukitt (O. Kindler), single myofibers were mounted with Vectashield Mounting Medium with DAPI (H-1200; Vector) and both were observed through a Zeiss microscope.

Immunohistochemistry and immunocytochemistry

Frozen sections (7-10 µm) and cultured cells were fixed with 4% PFA at room temperature for 5 min, permeabilized with 0.5% Triton X-100 for 5 min and blocked with 10% BSA for 30 min. Samples were incubated with primary antibody overnight at 4°C followed by secondary antibodies for 45 min at 37°C, then fluorochrome-conjugated streptavidin for 45 min at 37°C when necessary, and finally mounted with Vectashield Mounting Medium with DAPI and observed through epifluorescence or confocal Zeiss microscope.

The immunofluorescence staining was carried out with primary antibodies recognizing NG2 (AB5320; Chemicon Millipore; 1:200), αSMA (ab5694; Abcam; 1:100), PDGFRβ (#3169; Cell Signaling; 1:100), CD146 (ab75769; Abcam; 1:100), CD31 (ab7388; Abcam; 1:50 or M0823; Dako; 1:50), CD34 (14-0341-82; eBioscience; 1 µg/100 µl), CD45 (550539; BD Pharmingen; 1:50), NCAM/CD56 (123C3; Monosan; 1:50), PAX7 (DSHB; 1:50), MYOD1 (M3512; Dako; 1:50), myogenin (M3559; Dako; 1:50), MHC (MAB4470; R&D Systems; 1:20), KI67 (ab16667; Abcam; 1:500), nestin (ab81755; Abcam; 1:500), desmin (ab8592; Abcam; 1:100), laminin α1 (ab14055; Abcam; 1:500) and merosin/laminin α2 (MAB1922; Chemicon Millipore; 1:200). PAX7 immunostaining of mSCs was performed according to the M.O.M. Kit (BMK-2202; Vector). Visualization was carried out using the following secondary antibodies: Cy3-conjugated anti-mouse (715-166-150; Jackson), FITC-conjugated anti-rabbit (711-166-152; Jackson), Alexa Fluor 647 anti-chicken (A21449; Life Technologies) and biotinylated anti-rat (BA9401; Vector) coupled to Cy3-conjugated streptavidin (016-160-084; Jackson), a DAB detection Kit (SK-4100; Vector) or a Red Alkaline Phosphatase substrate kit (SK-51000; Vector).

Quantitative real-time PCR

Total RNAs were extracted from human cells by RNeasy Micro Kit (74004; Qiagen) and converted into double-strand complementary DNA using SuperScript III RT (18080-093; Life Technologies), according to the manufacturer's instructions. Real-time quantitative PCR was carried out on cDNA using 7900HT Fast Real-Time PCR System (Applied Biosystems). Each cDNA sample was amplified in triplicate by using the Platinum SYBR Green qPCR SuperMix-UDG (11733-038; Life Technologies). Analysis was carried out with the following primers: human β-actin (forward, CTGGGACGACATGGAGAAAA; reverse, AAGGAAGGCTGGAA-GAGTGC), human PAX7 (forward, CCCCCGCACGGGATT; reverse, TATCTTGTGGCGGATGTGGTT), human MYOD11 (forward, GACGG-CTCTCTCTGCTCCTTT; reverse, TCGAAACACGGGTCGTCATA) and human myogenin (forward, CACCCTGCTCAACCCCA; reverse, CACTGCCCCACTCTGGACT).

Protein array

One hundred and twenty cytokines were analyzed by protein array on 48 h-conditioned media from EC, pericytes and pericytes+EC cultures (triplicate for each medium and cytokine), according to the manufacturer's instructions accompanying the RayBio Human Cytokine Antibody Array (AAH-CYT-G1000; RayBiotech). ANGPT1 and ANGPT2 were analyzed by ELISA (DANG10 and DANG20, respectively; R&D Systems). ANGPT2 was also analyzed by the RayBio protein array and ANGPT1 levels could be converted into RayBio arbitrary units using a rule of 3.

RNA profiling

RNA profiling was carried out on human MPC using cDNA Array (R&D Systems) of 397 genes (Christov et al., 2007) and on post-natal $PAX3^{GFP/+}$ mSCs using Affymetrix Mouse Genome 430 2.0 Arrays. The data are available at GEO under accession GSE65927. To analyze the pathway enrichment, Gene Ontology (http://www.geneontology.org) and the murine KEGG pathways (www.genome.jp/kegg) were used.

Statistical analyses

The number of biological and technical replicates per point was always n=3 or more when indicated. All data are expressed as mean±s.e.m. Depending

Development (2015) 142, 1242-1253 doi:10.1242/dev.115386

on the experiments, unpaired Student's *t*-test and ANOVA tests were used. $P<0.05$ was considered significant.

Acknowledgements
We thank Barbara Gayraud-Morel, Pierre Rocheteau and Fabrice Chrétien (Pasteur Institute, France) for useful advice.

Competing interests
The authors declare no competing or financial interests.

Author contributions
E.K. carried out most of the experiments and analyses. Y.B.-A. purified human pericytes and MPCs. S.A.-M. performed RNA profiling. P.N. helped with *in vivo* experiments. F.R. provided expert advice on experiments. P.L. was responsible for animal reproduction, helped with *in vivo* experiments, performed single myofiber cultures, carried out analyses and designed figures. R.K.G. conceived the work and wrote the paper with E.K.

Funding
This study was supported by Association Française contre les Myopathies [15499, 15665 and 16803] and by Société Française de Myologie (awarded to E.K. in 2010). The transcriptome work was supported by funding to F.R. by Agence Nationale pour la Recherche (ANR) grant Epimuscle [# 11 BSV2 017 02] and Labex Revive. S.A.-M. received support from Association Institut de Myologie (AIM).

References

Abou-Khalil, R., Le Grand, F., Pallafacchina, G., Valable, S., Authier, F. J., Rudnicki, M. A., Gherardi, R. K., Germain, S., Chretien, F., Sotiropoulos, A. et al. (2009). Autocrine and paracrine angiopoietin 1/Tie-2 signaling promotes muscle satellite cell self-renewal. *Cell Stem Cell* **5**, 298-309.

Amos, P. J., Shang, H., Bailey, A. M., Taylor, A., Katz, A. J. and Peirce, S. M. (2008). IFATS collection: the role of human adipose-derived stromal cells in inflammatory microvascular remodeling and evidence of a perivascular phenotype. *Stem Cells* **26**, 2682-2690.

Arai, F., Hirao, A., Ohmura, M., Sato, H., Matsuoka, S., Takubo, K., Ito, K., Koh, G. Y. and Suda, T. (2004). Tie2/angiopoietin-1 signaling regulates hematopoietic stem cell quiescence in the bone marrow niche. *Cell* **118**, 149-161.

Armulik, A., Genové, G. and Betsholtz, C. (2011). Pericytes: developmental, physiological, and pathological perspectives, problems, and promises. *Dev. Cell* **21**, 193-215.

Arnold, L., Henry, A., Poron, F., Baba-Amer, Y., van Rooijen, N., Plonquet, A., Gherardi, R. K. and Chazaud, B. (2007). Inflammatory monocytes recruited after skeletal muscle injury switch into antiinflammatory macrophages to support myogenesis. *J. Exp. Med.* **204**, 1057-1069.

Beauchamp, J. R., Heslop, L., Yu, D. S. W., Tajbakhsh, S., Kelly, R. G., Wernig, A., Buckingham, M. E., Partridge, T. A. and Zammit, P. S. (2000). Expression of CD34 and Myf5 defines the majority of quiescent adult skeletal muscle satellite cells. *J. Cell Biol.* **151**, 1221-1234.

Birbrair, A., Zhang, T., Wang, Z.-M., Messi, M. L., Enikolopov, G. N., Mintz, A. and Delbono, O. (2013). Skeletal muscle pericyte subtypes differ in their differentiation potential. *Stem Cell Res.* **10**, 67-84.

Bloch, E. H. and Iberall, A. S. (1982). Toward a concept of the functional unit of mammalian skeletal muscle. *Am. J. Physiol.* **242**, R411-R420.

Bondjers, C., He, L., Takemoto, M., Norlin, J., Asker, N., Hellström, M., Lindahl, P. and Betsholtz, C. (2006). Microarray analysis of blood microvessels from PDGF-B and PDGF-Rbeta mutant mice identifies novel markers for brain pericytes. *FASEB J.* **20**, 1703-1705.

Bröhl, D., Vasyutina, E., Czajkowski, M. T., Griger, J., Rassek, C., Rahn, H.-P., Purfürst, B., Wende, H. and Birchmeier, C. (2012). Colonization of the satellite cell niche by skeletal muscle progenitor cells depends on Notch signals. *Dev. Cell* **23**, 469-481.

Buch, T., Heppner, F. L., Tertilt, C., Heinen, T. J. A. J., Kremer, M., Wunderlich, F. T., Jung, S. and Waisman, A. (2005). A Cre-inducible diphtheria toxin receptor mediates cell lineage ablation after toxin administration. *Nat. Methods* **2**, 419-426.

Chazaud, B., Sonnet, C., Lafuste, P., Bassez, G., Rimaniol, A. C., Poron, F., Authier, F. J., Dreyfus, P. A. and Gherardi, R. K. (2003). Satellite cells attract monocytes and use macrophages as a support to escape apoptosis and enhance muscle growth. *J. Cell Biol.* **163**, 1133-1143.

Chehrehasa, F., Meedeniya, A. C. B., Dwyer, P., Abrahamsen, G. and Mackay-Sim, A. (2009). EdU, a new thymidine analogue for labelling proliferating cells in the nervous system. *J. Neurosci. Methods* **177**, 122-130.

Christov, C., Chretien, F., Abou-Khalil, R., Bassez, G., Vallet, G., Authier, F.-J., Bassaglia, Y., Shinin, V., Tajbakhsh, S., Chazaud, B. et al. (2007). Muscle satellite cells and endothelial cells: close neighbors and privileged partners. *Mol. Biol. Cell* **18**, 1397-1409.

Coultas, L., Chawengsaksophak, K. and Rossant, J. (2005). Endothelial cells and VEGF in vascular development. *Nature* **438**, 937-945.

Crisan, M., Yap, S., Casteilla, L., Chen, C.-W., Corselli, M., Park, T. S., Andriolo, G., Sun, B., Zheng, B., Zhang, L. et al. (2008). A perivascular origin for mesenchymal stem cells in multiple human organs. *Cell Stem Cell* **3**, 301-313.

De Smet, F., Segura, I., De Bock, K., Hohensinner, P. J. and Carmeliet, P. (2009). Mechanisms of vessel branching: filopodia on endothelial tip cells lead the way. *Arterioscler. Thromb. Vasc. Biol.* **29**, 639-649.

Dellavalle, A., Sampaolesi, M., Tonlorenzi, R., Tagliafico, E., Sacchetti, B., Perani, L., Innocenzi, A., Galvez, B. G., Messina, G., Morosetti, R. et al. (2007). Pericytes of human skeletal muscle are myogenic precursors distinct from satellite cells. *Nat. Cell Biol.* **9**, 255-267.

Dellavalle, A., Maroli, G., Covarello, D., Azzoni, E., Innocenzi, A., Perani, L., Antonini, S., Sambasivan, R., Brunelli, S., Tajbakhsh, S. et al. (2011). Pericytes resident in postnatal skeletal muscle differentiate into muscle fibres and generate satellite cells. *Nat. Commun.* **2**, 499.

Duan, C., Ren, H. and Gao, S. (2010). Insulin-like growth factors (IGFs), IGF receptors, and IGF-binding proteins: roles in skeletal muscle growth and differentiation. *Gen. Comp. Endocrinol.* **167**, 344-351.

Franco, M., Roswall, P., Cortez, E., Hanahan, D. and Pietras, K. (2011). Pericytes promote endothelial cell survival through induction of autocrine VEGF-A signaling and Bcl-w expression. *Blood* **118**, 2906-2917.

Gitiaux, C., Kostallari, E., Lafuste, P., Authier, F.-J., Christov, C. and Gherardi, R. K. (2013). Whole microvascular unit deletions in dermatomyositis. *Ann. Rheum. Dis.* **72**, 445-452.

Guardiola, O., Lafuste, P., Brunelli, S., Iaconis, S., Touvier, T., Mourikis, P., De Bock, K., Lonardo, E., Andolfi, G., Bouche, A. et al. (2012). Cripto regulates skeletal muscle regeneration and modulates satellite cell determination by antagonizing myostatin. *Proc. Natl. Acad. Sci. USA* **109**, E3231-E3240.

Jeansson, M., Gawlik, A., Anderson, G., Li, C., Kerjaschki, D., Henkelman, M. and Quaggin, S. E. (2011). Angiopoietin-1 is essential in mouse vasculature during development and in response to injury. *J. Clin. Invest.* **121**, 2278-2289.

Kunisaki, Y., Bruns, I., Scheiermann, C., Ahmed, J., Pinho, S., Zhang, D., Mizoguchi, T., Wei, Q., Lucas, D., Ito, K. et al. (2013). Arteriolar niches maintain haematopoietic stem cell quiescence. *Nature* **502**, 637-643.

Leatherman, J. (2013). Stem cells supporting other stem cells. *Front. Genet.* **4**, 257.

Lescaudron, L., Peltékian, E., Fontaine-Pérus, J., Paulin, D., Zampieri, M., Garcia, L. and Parrish, E. (1999). Blood borne macrophages are essential for the triggering of muscle regeneration following muscle transplant. *Neuromuscul. Disord.* **9**, 72-80.

Liu, J.-L., Grinberg, A., Westphal, H., Sauer, B., Accili, D., Karas, M. and LeRoith, D. (1998). Insulin-like growth factor-I affects perinatal lethality and postnatal development in a gene dosage-dependent manner: manipulation using the Cre/loxP system in transgenic mice. *Mol. Endocrinol.* **12**, 1452-1462.

Lu, H., Huang, D., Saederup, N., Charo, I. F., Ransohoff, R. M. and Zhou, L. (2011). Macrophages recruited via CCR2 produce insulin-like growth factor-1 to repair acute skeletal muscle injury. *FASEB J.* **25**, 358-369.

Maisonpierre, P. C., Suri, C., Jones, P. F., Bartunkova, S., Wiegand, S. J., Radziejewski, C., Compton, D., McClain, J., Aldrich, T. H., Papadopoulos, N. et al. (1997). Angiopoietin-2, a natural antagonist for Tie2 that disrupts in vivo angiogenesis. *Science* **277**, 55-60.

Mathew, S. J., Hansen, J. M., Merrell, A. J., Murphy, M. M., Lawson, J. A., Hutcheson, D. A., Hansen, M. S., Angus-Hill, M. and Kardon, G. (2011). Connective tissue fibroblasts and Tcf4 regulate myogenesis. *Development* **138**, 371-384.

McCarthy, J. J., Srikuea, R., Kirby, T. J., Peterson, C. A. and Esser, K. A. (2012). Inducible Cre transgenic mouse strain for skeletal muscle-specific gene targeting. *Skelet. Muscle* **2**, 8.

Méndez-Ferrer, S., Michurina, T. V., Ferraro, F., Mazloom, A. R., MacArthur, B. D., Lira, S. A., Scadden, D. T., Ma'ayan, A., Enikolopov, G. N. and Frenette, P. S. (2010). Mesenchymal and haematopoietic stem cells form a unique bone marrow niche. *Nature* **466**, 829-834.

Morgan, J. and Muntoni, F. (2007). Mural cells paint a new picture of muscle stem cells. *Nat. Cell Biol.* **9**, 249-251.

Murphy, M. M., Lawson, J. A., Mathew, S. J., Hutcheson, D. A. and Kardon, G. (2011). Satellite cells, connective tissue fibroblasts and their interactions are crucial for muscle regeneration. *Development* **138**, 3625-3637.

Ozerdem, U., Grako, K. A., Dahlin-Huppe, K., Monosov, E. and Stallcup, W. B. (2001). NG2 proteoglycan is expressed exclusively by mural cells during vascular morphogenesis. *Dev. Dyn.* **222**, 218-227.

Pasut, A., Jones, A. E. and Rudnicki, M. A. (2013). Isolation and culture of individual myofibers and their satellite cells from adult skeletal muscle. *J. Vis. Exp.* e50074.

Rajantie, I., Ilmonen, M., Alminaite, A., Ozerdem, U., Alitalo, K. and Salven, P. (2004). Adult bone marrow-derived cells recruited during angiogenesis comprise precursors for periendothelial vascular mural cells. *Blood* **104**, 2084-2086.

Relaix, F., Rocancourt, D., Mansouri, A. and Buckingham, M. (2005). A Pax3/Pax7-dependent population of skeletal muscle progenitor cells. *Nature* **435**, 948-953.

Rojas-Ríos, P. and González-Reyes, A. (2014). Concise review: the plasticity of stem cell niches: a general property behind tissue homeostasis and repair. *Stem Cells* **32**, 852-859.
Rosen, G. D., Sanes, J. R., LaChance, R., Cunningham, J. M., Roman, J. and Dean, D. C. (1992). Roles for the integrin VLA-4 and its counter receptor VCAM-1 in myogenesis. *Cell* **69**, 1107-1119.
Rosenblatt, J. D., Lunt, A. I., Parry, D. J. and Partridge, T. A. (1995). Culturing satellite cells from living single muscle fiber explants. *In Vitro Cell. Dev. Biol. Anim.* **31**, 773-779.
Sallum, A. M., Varsani, H., Holton, J. L., Marie, S. K. and Wedderburn, L. R. (2013). Morphometric analyses of normal pediatric brachial biceps and quadriceps muscle tissue. *Histol. Histopathol.* **28**, 525-530.
Shepro, D. and Morel, N. M. (1993). Pericyte physiology. *FASEB J.* **7**, 1031-1038.
Shim, W. S. N., Ho, I. A. W. and Wong, P. E. H. (2007). Angiopoietin: a TIE(d) balance in tumor angiogenesis. *Mol. Cancer Res.* **5**, 655-665.
Sonnet, C., Lafuste, P., Arnold, L., Brigitte, M., Poron, F., Authier, F., Chrétien, F., Gherardi, R. K. and Chazaud, B. (2006). Human macrophages rescue myoblasts and myotubes from apoptosis through a set of adhesion molecular systems. *J. Cell Sci.* **119**, 2497-2507.
Soriano, P. (1999). Generalized lacZ expression with the ROSA26 Cre reporter strain. *Nat. Genet.* **21**, 70-71.
Stratman, A. N., Malotte, K. M., Mahan, R. D., Davis, M. J. and Davis, G. E. (2009). Pericyte recruitment during vasculogenic tube assembly stimulates endothelial basement membrane matrix formation. *Blood* **114**, 5091-5101.
Thomas, M. and Augustin, H. G. (2009). The role of the Angiopoietins in vascular morphogenesis. *Angiogenesis* **12**, 125-137.
Tonlorenzi, R., Dellavalle, A., Schnapp, E., Cossu, G. and Sampaolesi, M. (2007). Isolation and characterization of mesoangioblasts from mouse, dog, and human tissues. *Curr. Protoc. Stem Cell Biol.* Chapter 2, Unit 2B 1.
Tozer, S., Bonnin, M.-A., Relaix, F., Di Savino, S., Garcia-Villalba, P., Coumailleau, P. and Duprez, D. (2007). Involvement of vessels and PDGFB in muscle splitting during chick limb development. *Development* **134**, 2579-2591.
Valable, S., Bellail, A., Lesne, S., Liot, G., Mackenzie, E. T., Vivien, D., Bernaudin, M. and Petit, E. (2003). Angiopoietin-1-induced PI3-kinase activation prevents neuronal apoptosis. *FASEB J.* **17**, 443-445.
Wakui, S., Yokoo, K., Muto, T., Suzuki, Y., Takahashi, H., Furusato, M., Hano, H., Endou, H. and Kanai, Y. (2006). Localization of Ang-1, -2, Tie-2, and VEGF expression at endothelial-pericyte interdigitation in rat angiogenesis. *Lab. Invest.* **86**, 1172-1184.
White, R. B., Biérinx, A.-S., Gnocchi, V. F. and Zammit, P. S. (2010). Dynamics of muscle fibre growth during postnatal mouse development. *BMC Dev. Biol.* **10**, 21.
Williams, R. S. and Annex, B. H. (2004). Plasticity of myocytes and capillaries: a possible coordinating role for VEGF. *Circ. Res.* **95**, 7-8.
Yin, H., Price, F. and Rudnicki, M. A. (2013). Satellite cells and the muscle stem cell niche. *Physiol. Rev.* **93**, 23-67.
Zammit, P. S., Golding, J. P., Nagata, Y., Hudon, V., Partridge, T. A. and Beauchamp, J. R. (2004). Muscle satellite cells adopt divergent fates: a mechanism for self-renewal? *J. Cell Biol.* **166**, 347-357.
Zhu, X., Hill, R. A. and Nishiyama, A. (2008). NG2 cells generate oligodendrocytes and gray matter astrocytes in the spinal cord. *Neuron Glia Biol.* **4**, 19-26.